**Title**
DELAY LINE PROPORTIONAL CHAMBERS FOR THE FERMILAB EXTERNAL MUON IDENTIFIER



**Author**
Parker, Sherwood

**Publication Date**
1977-10-01

Presented at the IEEE Symposium on
Nuclear Science, San Francisco, CA,
October 19 - 21, 1977

LBL-6776
UH 511-259-77



# DELAY LINE PROPORTIONAL CHAMBERS FOR THE FERMILAB EXTERNAL MUON IDENTIFIER

Sherwood Parker, John Orthel, and John Marriner

October 19, 1977

Prepared for the U. S. Department of Energy
under Contract W-7405-ENG-48



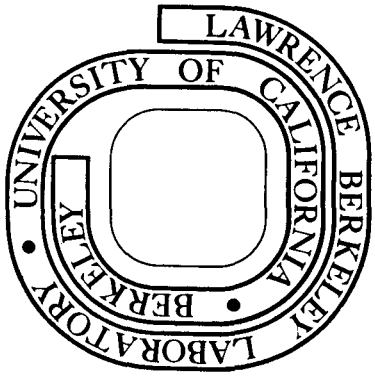

## DISCLAIMER

# DELAY LINE PROPORTIONAL CHAMBERS FOR THE FERMILAB EXTERNAL MUON IDENTIFIER

Sherwood Parker,* John Orthel,† and John Marriner†
Lawrence Berkeley Laboratory
University of California
Berkeley, California

## Summary

Thirty nine, one meter square proportional chambers with delay line readout have been constructed for the external muon identifier of the Fermilab 15 foot bubble chamber. They provide X,Y,U(45°) and T (avalanche time) information using a single wire plane, etched strip cathodes and nine amplifiers. They have a time resolution of ±27ns, single particle spatial resolution of ±2 to ±3mm and double particle resolution of ~2 1/2 to 4cm. The energy accessable to each wire is limited so none of the wires in the first 25 chambers has broken since their installation in 1973-4.

## Introduction

In designing detectors for an external muon identifier to operate behind the Fermilab 15 foot bubble chamber, we had to satisfy the following requirements:

1. Large area ($24m^2$ initially, now $39m^2$),
2. Spatial resolution < ±5mm,
3. Operate in a 5-10KG, non-unfirom magnetic fringe field from the bubble chamber,
4. Sensitive for > 1m second,
5. Inexpensive,
6. High data rates not necessary. (The detectors operate in a neutrino beam with a one kilometer beam shielding the bubble chamber from the primary beam. Several meters of additional absorber stop of scatter most hadrons leaving the bubble chamber, permitting the identification of muons which do not interact strongly.)

Requirements 1, 2, and 3 eliminated scintillator hodocopes, 3 eliminated drift chambers, 4 eliminated spark chambers since they have memory times of only ~1 μsec before the high voltage pulse and recovery times of ~ 1-10 msec while 5 made it almost impossible to build one-amplifier-per-wire (or wire group) proportional chambers with anything like the required spatial resolution. However 6 made possible the use of electromagnetic delay line readout,[2] a technique developed by Victor Perez-Mendez.[3]

The chambers in use at Fermilab, by exploiting fully a number of useful properties of delay lines, provide from each chamber, containing only one wire plane, X,Y,U (45°), and T (avalanche time) information.

## Construction

Figure 1 shows an exploded, schematic view of a chamber and associated readout. The wire (Y) plane is of 20 μm stainless steel (first 25 chambers, installed starting in 1973) or gold plates tungsten (last 14 chambers, installed in 1977) with 5 mm separation. The cathode planes (X and U) are gold plated strips of 34 μm thick copper on a Mylar backing which is glued to 1.9 ×11.7×111.7 cm Hexcel support panels. (See Figure 2). The 6-10 frames are glued directly to the cathode planes which extend beyond them to reach the delay lines and thick film resistors (baked on G-10) that complete the DC circuit. The anode wires are glued to the bottom frame and soldered to a copper-Mylar sheet glued to the same frame. The two halves are bolted together, compressing an O-ring which presses on the copper-Mylar sheet, not on the wires. No machined O-ring grooves are needed; just some 1 mm thick, sheared G-10 stripes which are glued to the top frame.

The external circuit connections are also simple. The delay lines are capacitatively coupled. A sandwich, consisting of (1) a phenolic platform, (2) foam rubber, (3) the copper-Mylar sheet, (4) the connecting thick film resistor strip and the delay line, (5) more foam rubber, and (6) another phenolic piece is compressed by screws attached to the aluminum housing box. The adjustment is not at all critical. Two sheets of 25 μm Mylar are placed between the anode connecting sheet, which is at high voltage, and its delay line. We found it necessary to solder on the anode thick-film resistors. Figure 3 shows an assembled chamber with part of the aluminum box top removed to show the delay lines and phenolic pressure pads.

## Delay Lines

Figure 4 shows a schematic view of a delay line. Charge of one sign moves slowly along the ground strips with a velocity $v = (L'C')^{-1/2}$ where L' and C' are the inductance and capacitance per unit length. Equal charge of the opposite sign moves along the windings with a velocity v/(average pitch angle) generating a magnetic field that reaches out ahead and behind by a distance comparable to the smallest transverse dimension of the line, h. L' remains proportional to the number of turns per unit length squared, $n'^2$, only so long as the current is in phase over a length greater than the transverse dimensions of the delay line. At high frequencies this is no longer so, and the decrease in $L'(\omega)$ causes an increase in $v(\omega)$ and a dispersion of the pulse. Figure 5 shows the effects of such dispersion. It can be removed with the floating patch compensation strips shown in Figure 3[1,2] whose projected length along the delay line axis is comparable to its transverse dimensions. Their potential is an average of that of the windings passing over them. For $\lambda = v/\omega << h$, this is close to ground and so the strips cause an increase in effective ground area and hence in $C'(\omega)$ sufficient to keep L'C' nearly constant.

Figure 6 shows how pulses are capacitatively coupled into the delay lines. Indicated schematically are the ground strip, bottom part of the windings (in cross-section) and connecting strips from the chamber, roughly that part of Figure 4 under the words "signal propagation." After charges appear (4a) on the connecting strip due to the positive ions drifting away from the avalanche region, charge of the opposite sign moves rapidly up the low impedance ground strip (4b). The windings, isolated by their high inductance, and separated from the ground strip by an extra 25 μm layer of Kapton come to about 70% of the coupling strip potential. As only 5% of the lines of force pass between the copper of the windings, most of the energy is transferred to the delay line and to the two pulses that travel out from the point of injection (4c). This efficient coupling first became apparent to us when we made our first experimental chamber with cathode strips

at 27° (instead of 45°) having central region that coupled to two delay lines.[4] As we moved a source past the border into the central region, the delay line signal dropped abruptly to half its original value.

In addition to delayed signals from amplifiers on each end of the delay lines, we get a prompt (avalanche time) signal by inserting a current amplifier in series with the incoming ground current out from the point of injection (c). This efficient coupling first became apparent to us when we made our first experimental chamber with cathode strips at 27° (instead of 45°) having a central region that coupled to two delay lines. As we moved a source past the border to the central region, the delay line signal dropped abruptly to half its original value.

In addition to delayed signals from amplifiers on each end of the delay lines we get a prompt (avalanche time) signal by inserting a current amplifier in series with the incoming ground current (Figure 6a) of the anode delay line between box ground and delay line ground. No prompt signal appears at the delayed signal amplifier inputs since they are differentially connected between the delay line (not box) ground and the windings and because of the low input impedance of the current amplifier.

A single particle traversing the chamber away from the 45° UA-UB border will produce seven pulses - one at each end of the X,Y, and UA or UB delay lines and a T pulse. Since we are only determining three things, X, Y, and time, we have a 4-C fit. (The first group of chambers had only one amplifier on UA and UB delay lines and provided 3-C fits. They are now being upgraded). In addition to helping maintain high efficiency, the extra constraints permit multiple track events to be unscrambled. Figure 7 shows how this can be done using a simplified example: one delay line with two delayed and one prompt outputs which determine X and time with a 1-C fit. Here the shaded circles representing three tracks, two simultaneous and one delayed, are separable from the open ones representing spurious solutions since only the former are at triple crossings. In actual practice, in our experiment, there are too many accidental, spurious 1-C fits, and we require at least 2-C.

Figure 8 uses delayed sweeps to show the detailed structure of anode and cathode outputs from a $^{55}Fe$ source. As the source makes tracks only about 100 μm long, the position quantization of the anode wires and the continuous nature of the cathode readout are clearly evident. Tracks crossing the entire gap at an angle of more than about 15° will usually send their ionization across two or more wires. Since the delay line pulses are wider than the wire to wire spacing, the injected pulses are added in an analog fashion, producing a peak that follows the track centroid location in a continuous fashion (subject of course to ionization fluctuations). A delay line chamber tilted at an appropriate angle to a particle beam will thus provide a continuous readout in both X and Y simultaneously.

Figure 9 shows $^{55}Fe$ pulses from the prompt and anode delay line amplifiers. The increased width and reduced amplitude of pulses from the far end of the line is not due to dispersion but to ohmic losses in the windings. As a pulse travels along the line, $q = \int i\,dt$ remains constant but the energy remaining that could flow into a matched terminating resistor, $\omega = \int i^2 Z_{term}\,dt$, decreases. When $\int i\,dt$ stays constant, and $\int i^2\,dt$ decreases, the current and hence voltage pulse must widen and decrease in peak height.

## Cathodes

The planar cathodes we used have several advantages and one unexpected danger. They simplify the chamber construction, keep it compact in the Z direction, provide their own readout connections, serve as the gas barrier, and permit the electric field at the cathode to be over 100 times lower than that at the anode. This, together with the fact that each strip (and anode wire) is fed with its own 5-10 MΩ thick film resistor and is coupled to the delay line through a capacitor of only ~100 pF insures the chambers from damage due to high voltage breakdown. In four years of use, none of the 5000 wires on the original 25 chambers have broken. With the cathodes and anode wires extending into the frames on all sides, no special precautions were necessary against edge breakdown. The chambers were sensitive to within ~ 1cm of the frames. On the other hand, some care must be taken to keep the cathodes flat to ~± 1/2mm, and we found a completely new (to us, anyway) kind of high voltage discharge when we tested the first chamber: one that came only in a magnetic field of about 1 KG or more. Tests indicated the pulses were located along an anode wire, would stop and invariably return when high voltage was turned off and on but would sometimes stop and not return when the magnetic field was turned off and on. Finally, when we found they could be modified by rotating the chamber in the magnetic field, it became clear that we had small bits of iron in the chamber which sometimes jumped up and followed the gradient until they hit the cathode plane, where they served as field emission points. Instructions to sweep production chambers with a magnet were not followed due to a misunderstanding, and 75% of all the chambers broke down when the 15' bubble chamber field was turned on for the first time. Burn out time for the first group of points was typically ~ 5-10 days and now it is rare to find a new piece of iron in any of the original chambers when the field is turned on. The second group were swept, small sub-millimeter particles were removed, and non have so far broken down due to the field. Chunks of iron aside, the chambers settle down, in a few hours to a few days, to counting rates of about 150-200 Hz, only slightly more than the cosmic ray rate.

## Box Electronics

Because of its location around a hydrogen bubble chamber over 100 m away from the control area and in a high magnetic field, we decided to restrict the electronics in the chamber housing box to (1) the delay lines and their nine amplifiers, (2) two I.C. chips to regulate and protect the low voltage (±12v), and (3) a fiducial driver. Discriminators, digitizers, and other electronics[5] was immediately accessable in our control area. The delay line amplifiers were designed by Kai Lee,[5] use a μA733 followed by an RC filter and a line driver, and, for the various lines, have gains from 750 to 2000. The prompt have an additional common base input stage to provide low input impedance and gives 1V out for about 3 μA in.

Because track coordinates are over-determined, fiducials are not essential either in routine data collection or in calibration, however they do provide a useful calibration check as well as computer controlled monitoring of all system electronics. The fiducial circuit consists of an emitter follower driving a MECL chip which pulses an RC circuit that mimics chamber pulses. These signals are applied directly to the cathode strips entering at the edges of the gas volume and to the Mylar side of the corresponding anode connector strips.

The complete chamber electronics, delay lines and all, fit in a 6cm wide border. This was done to provide necessary overlap of the sensitive areas of

adjacent chambers in a rather constricted space on the outside of the spherical bubble chamber vacuum tank. We paid a fairly high price for this compact design, for the delay lines and associated chamber structures act as guides for waves that are not completely confined to the delay lines, and cross-coupling between adjacent structures, lines, amplifiers, and output cables can cause spurious pulses. In general, we know how to reduce the worst of these so the largest spurious signal from a $^{55}$Fe source on any given channel is less than 10% of the smallest valid signal.

Some sources of spurious signals are:

1. Reflections due to mismatched terminations. Sources of comparable importance include winding resistance which introduces an imaginary component in the line impedance, the frequency dependence of the real part $Z = \sqrt{L(\ )/c(\omega)}$ since $R_{term}$ is independent of $\omega$, amplifier input capacitance, and the decrease of L' near the ends of the line. Figure 10 shows an example of a reflection.
2. Cathode - cathode coupling is small because the delay lines soak up the energy and prevent large voltage excursions. However, a single grounded strip is necessary between the two halves of the U plane.
3. Cathode - anode coupling. Some care is needed here including DC grounding of cathode strips lying wholy in the G-10 frame, due to its high dielectric constant.
4. Discontinuities in cathode and anode planes. There is no problem if they are kept outboard of the delay line windings.
5. Dispersion. Only a problem near the ends of the anode line where high frequencies are present. Additional strips of narrow compensation are needed there for best results.
6. Delay line-delay line coupoing. The UA line is directly above XA and magnetic fields from one can induce pulses in the other. This is prevented by using a grounded shield between them and by having velocities which differ by a factor of 2.
7. Feedback and cross-coupling of amplified pulses. This is controlled by designing the amplifiers and output cables together with their associated grounds so that the currents flow close to each other, by careful grounding and shielding and by not using any more gain than necessary. This has given us the most trouble, by far. More room - even 20cm — and the use of a correspondingly larger box would have done wonders.

## Performance

Due to differences in the chamber structures to which they are complied, the 4 delay lines have different specifications. The first 25 chambers used lines with impedances of 1.0 kΩ (UA) to 1.7 kΩ (UB) delays of 3.5 μs (UA) to 12.5 μs (UB) and delay-to-rise time ratios of 22 (UA) to 31 (anode). Attenuation for $^{55}$Fe signals ranged from 0.2 (X cathode) to 0.4 (anode) and was about 0.5 for the more slowly rising pulses of crossing tracks. Figures 11, 12, and 13 show their time (±27 ns) and spatial (±2.2mm cathode, ±2.7mm anode) resolution measured in a pion beam using the 28 M $H_z$ digitizing electronics. Their efficiency as measured in this beam was 99±1%. Double pulse reolution could not be measured but estimated to be ~5cm by injecting a pulse from a part of the chamber to nearby wirer in another part.

The final group of chambers use delay lines with coarser wire (0.14mm vs 0.10mm diameter) to reduce ohmic losses and sufficiently larger cross sections (typically 8×60mm vs 5×30mm) so their delay now ranges from 8 μs (UA) to 17 μs (anode), reducing clock count distances by a factor of about two. The pulses are also narrower, and double pulse resolution on the anode line should range from 2-1/2cm at the near end, and 4cm in the middle, to 5-6 at the far end. Impedance and attenuation levels are about the same.

Measurements corresponding to Figures 11-13 have not yet been made. We hope to include them in a later report which will also give more detail on circuits, delay line design, and the methods that were used to remove spurious signals.

## Acknowledgements

Ron Jones participated in the design and construction of the half-meter prototype and made important contributions to the readout electronics. Norm Andersen and his group built all the chambers and supplied many ingenious ideas to help simplify their construction. Peter Harding made the final delay lines and a winding machine that uniformly wound its 6000 turns of fine wire in less than 10 minutes.

## Footnotes and References

*Department of Physics and Astronomy, University of Hawaii, Honolulu, HI 96822

†Lawrence Berkeley Laboratory, Berkeley, CA 94720

1. R. J. Cence, et al., Nucl. Instr. and Meth. 138 (1976) 245.
2. H. Kallmann, Proc. I.R.E. 34 (1946) 646.
3. V. Perez-Mendez, et al., Nucl. Instr. and Meth. 77 (1970) 325, 89 (1970) 257, 99 (1972) 381, 106 (1973) 407.
4. S. I. Parker and R. Jones, "External Muon Identifier Development: Half Meter Proportional Chamber Test Results" LBL-797, UH-511-122-72, May 1972.
5. E. Binnall, F. Kirsten, K. Lee, and C. Nunnally, IEEE Trans. or Nucl. Sci. NS-20 (1972) 367.

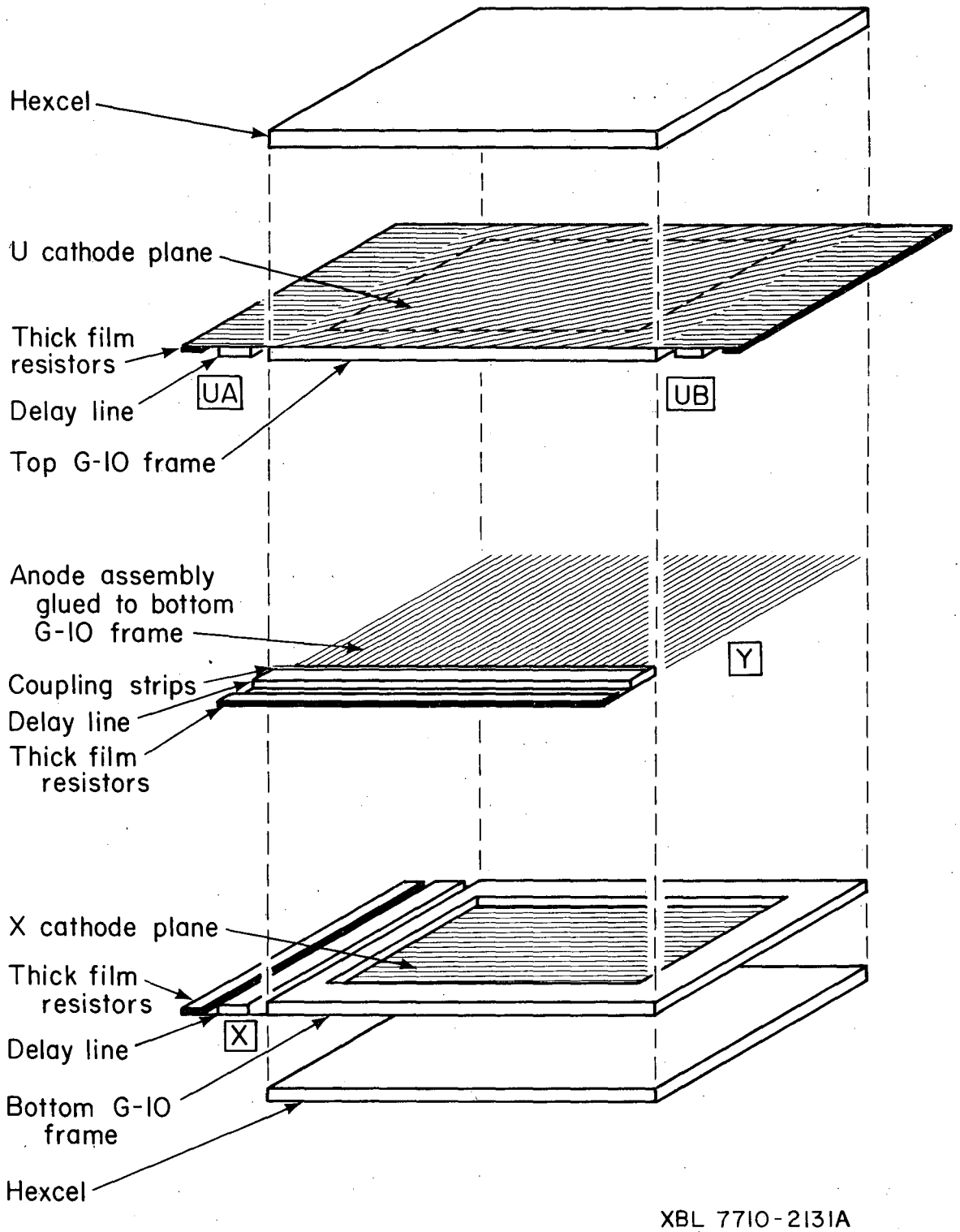


Fig. 1 Exploded, schematic view of chamber and readout.

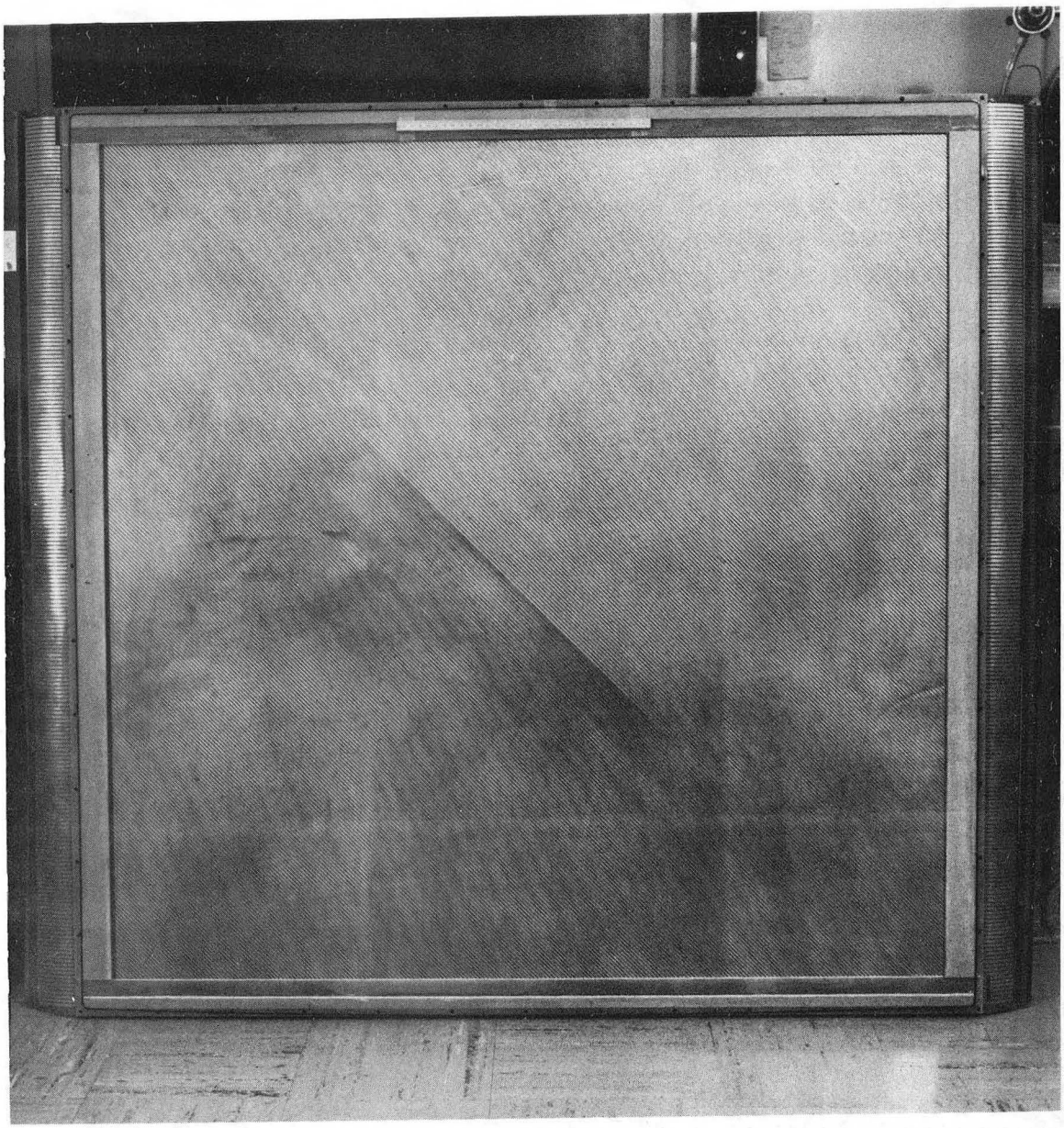

CBB 728-4281

Fig. 2. Cathode plane.

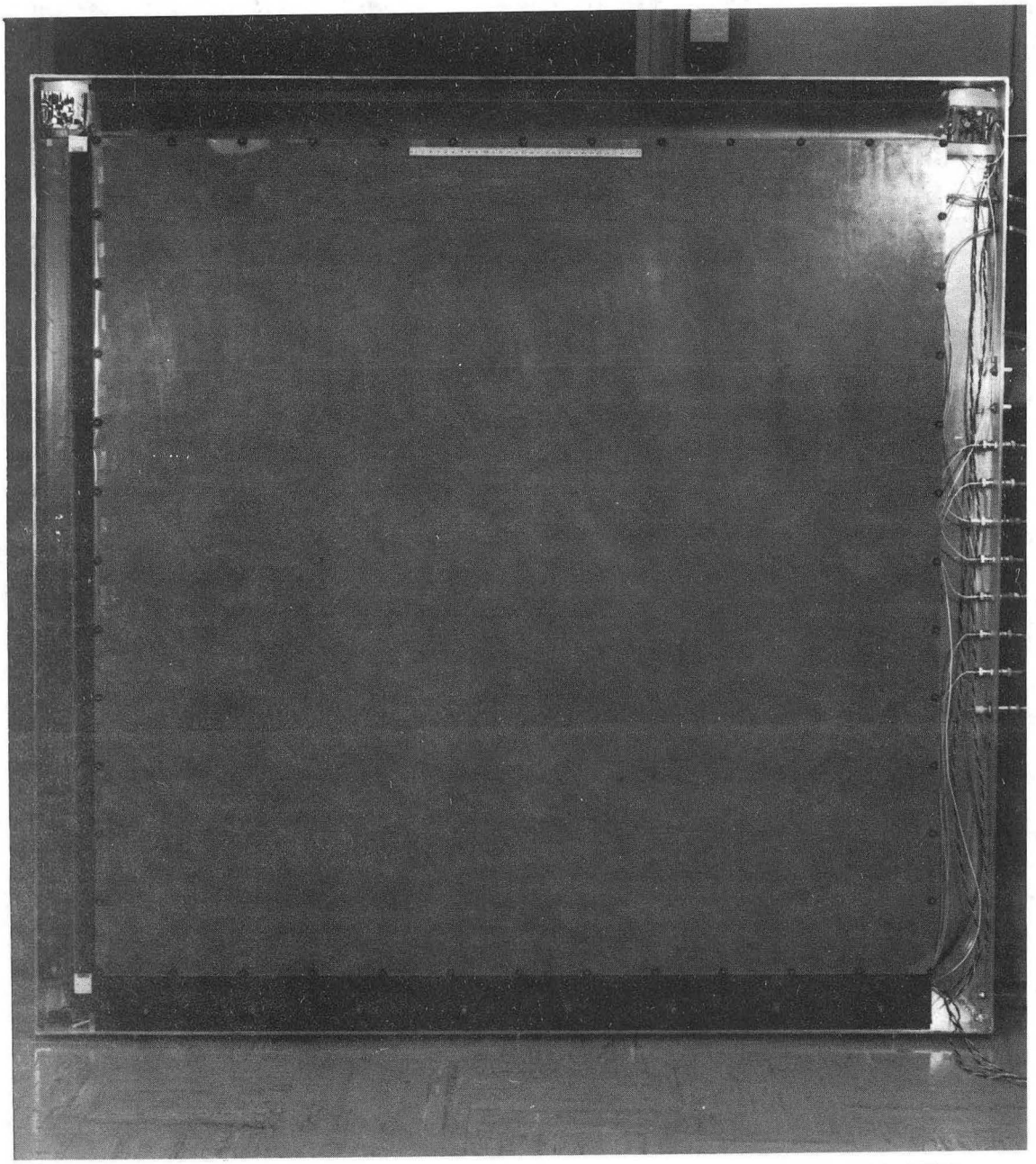

CBB 728-4285

Fig. 3. Assembled proportional chamber with housing box top removed. Visible at the left is a cathode plane, at the bottom a delay line, and at the right a phenolic pressure pad.

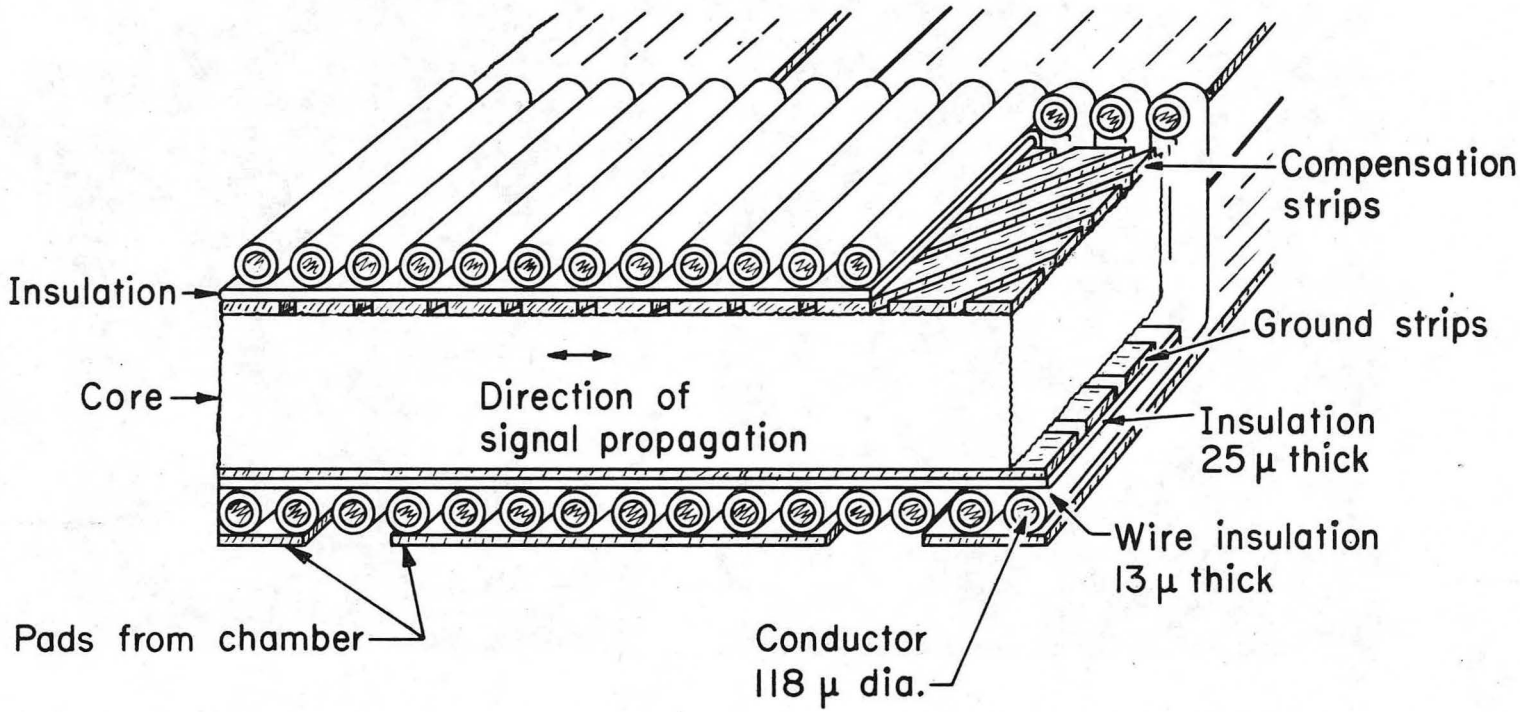


XBL725-2993

Fig. 4. Cross-section view of delay lines and connecting strips from chamber.

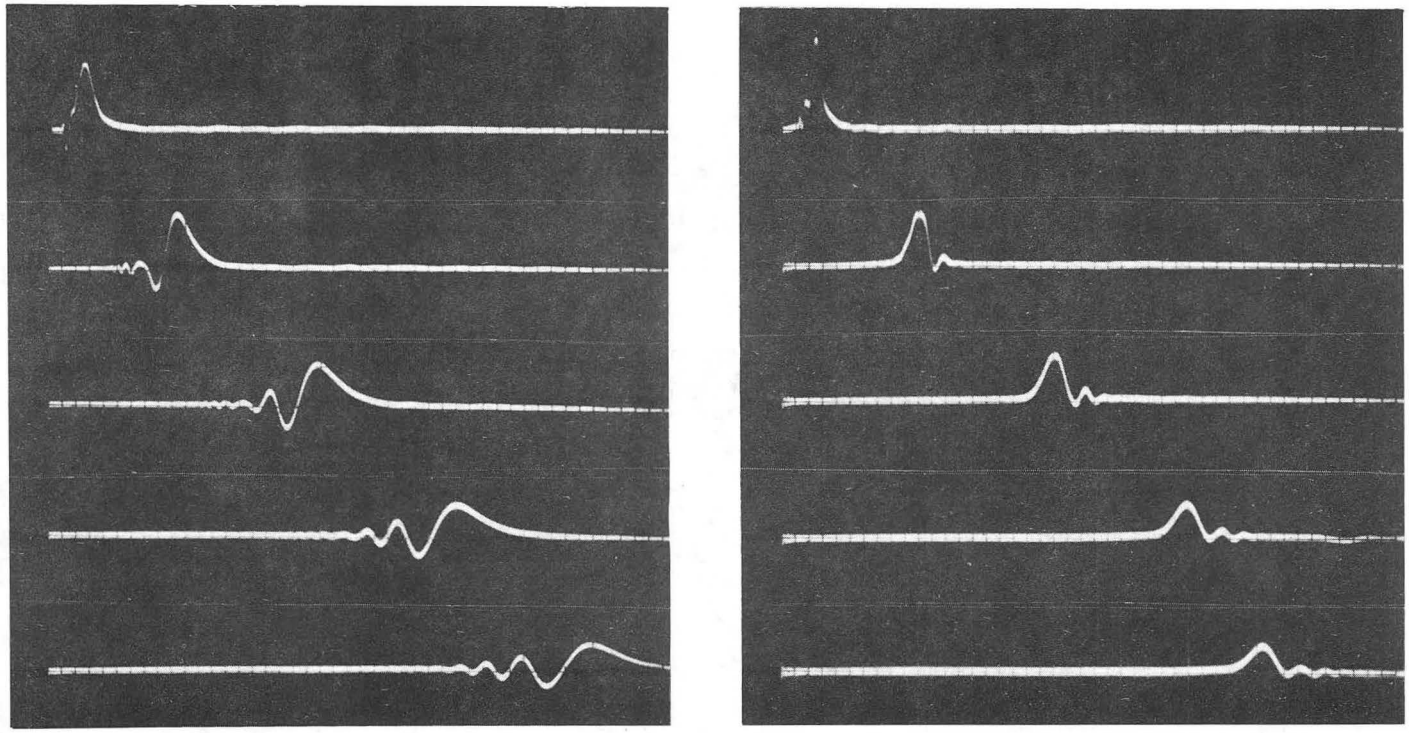

XBB 763-2750

a. b.

Fig. 5. Dispersion in uncompensated delay lines for signals capacitatively injected at increasing distances from the amplifier. (a) too little compensation, (b) too much. Sweep speed 1 μs/cm. The jog on each top trace is due to the pulser connection and is not present when a proportional chamber is the source.

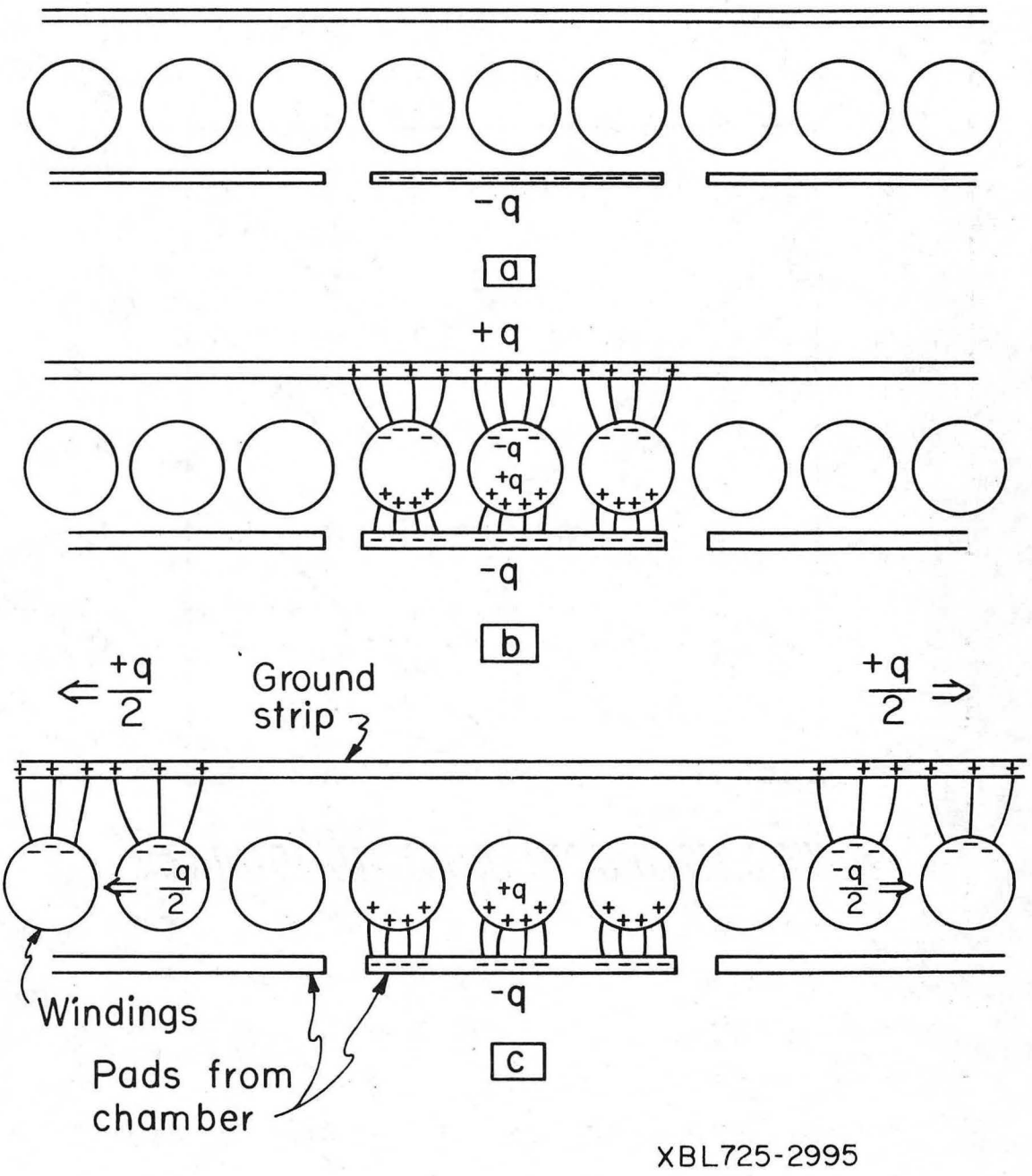


Fig. 6. Schematic cross section views of delay lines and chamber connecting strips. Charges that provide the DC chamber field are not shown.

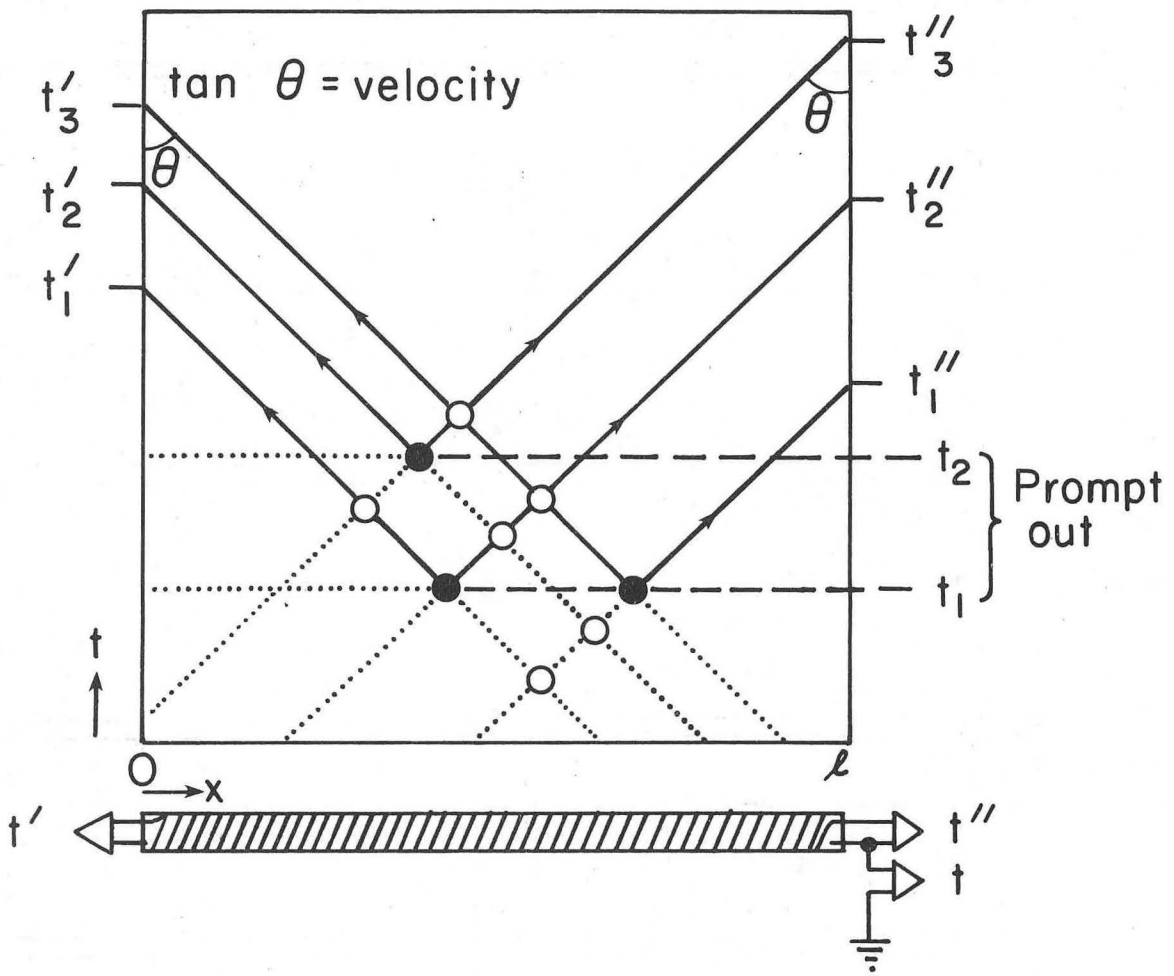


XBL 764-2725

Fig. 7. Space-time diagram for delay line signal propagation.

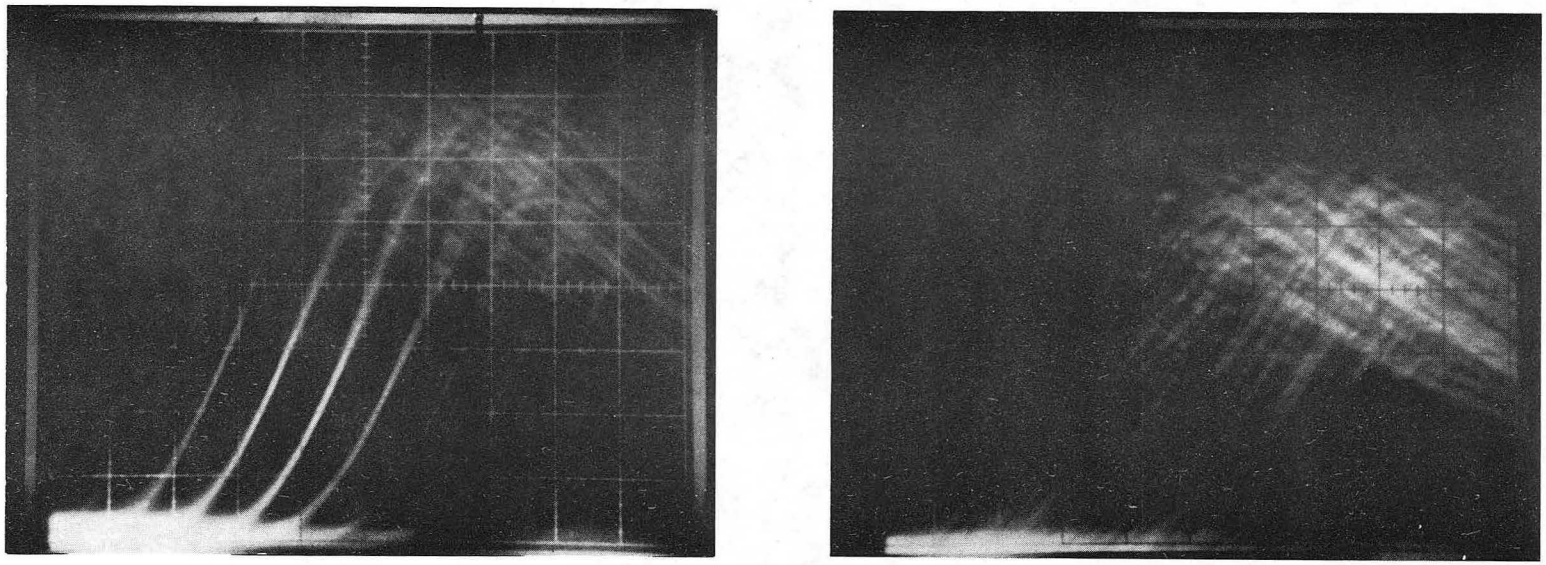


Fig. 8. Delayed signals from a $^{55}Fe$ source at the chamber edge seen at maximum delay. The structure in the anode signals is due to the entire region of ionization ( ~ 0.1mm long) being drawn to one or another anode wire. The non-zero width ($\sigma \approx \pm 0.3$mm after 1m output 100 ns/cm, 100 mV/cm.

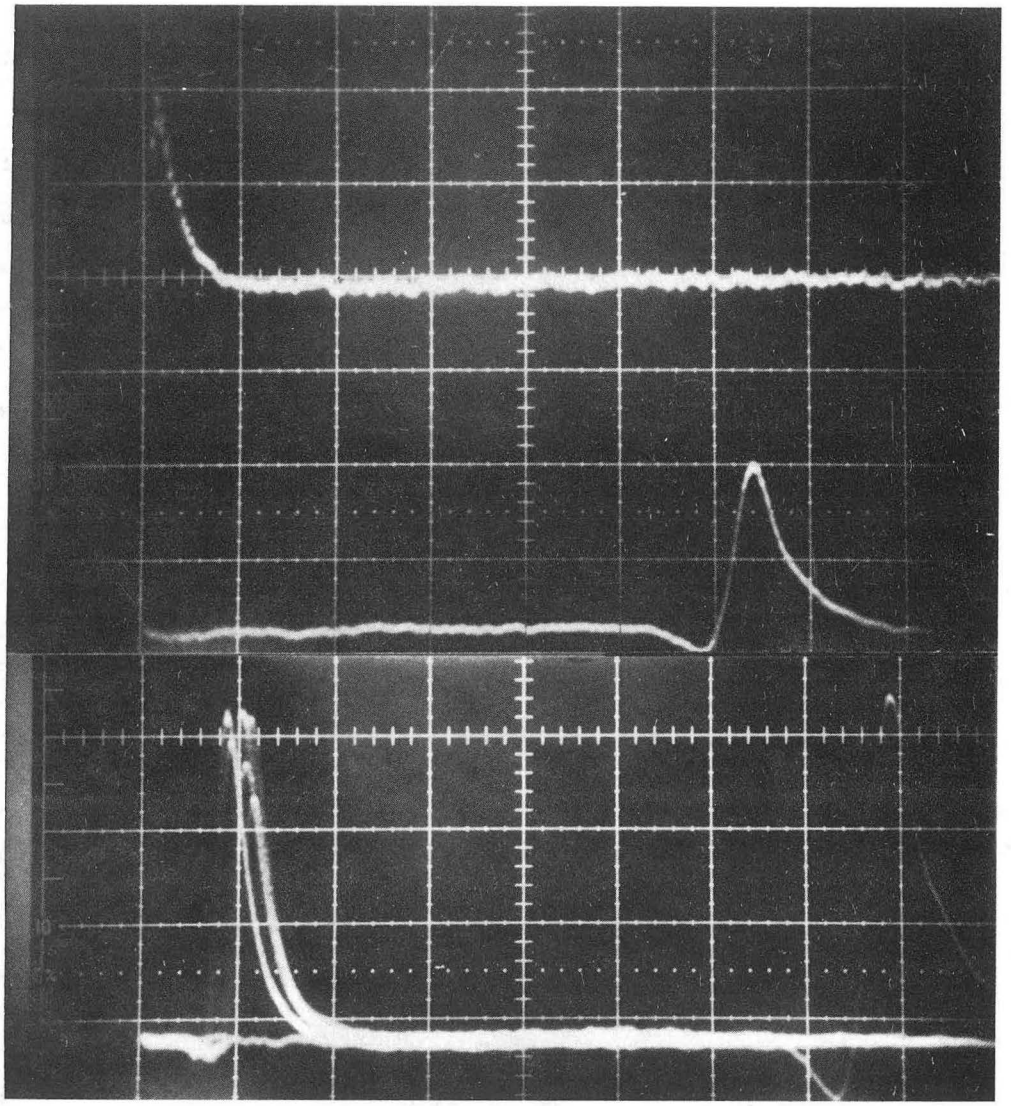

XBB 770-10700

Fig. 9. Anode delay line 0.2 v/cm, 2 μs/cm, $^{55}$Fe tope trace: prompt (triggers scope). Middle trace: delayed, $^{55}$Fe far. Bottom trace: delayed, $^{55}$Fe near-cosmic ray at far end also visible.

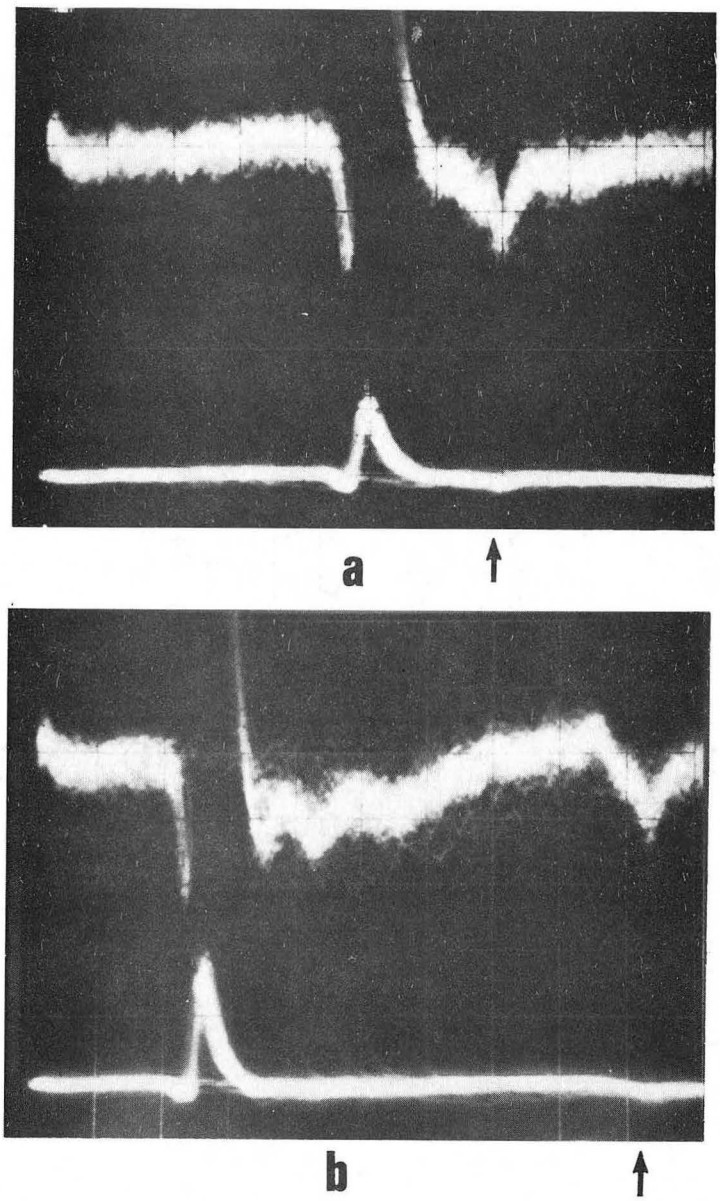


XBB 763-2755

Fig. 10. Reflection (↑) on x (cathode) delay line for source (a) near amplifier and (b) away from amplifier. The negative pulse at the leading edge of the main pulse is due to imperfect compensation and does not cause an extra count. Some amplifier ringing is also seen in (b). Prompt trigger, 2 μs/cm, 50 mV/cm (top trace), 500 mV/cm (bottom trace).

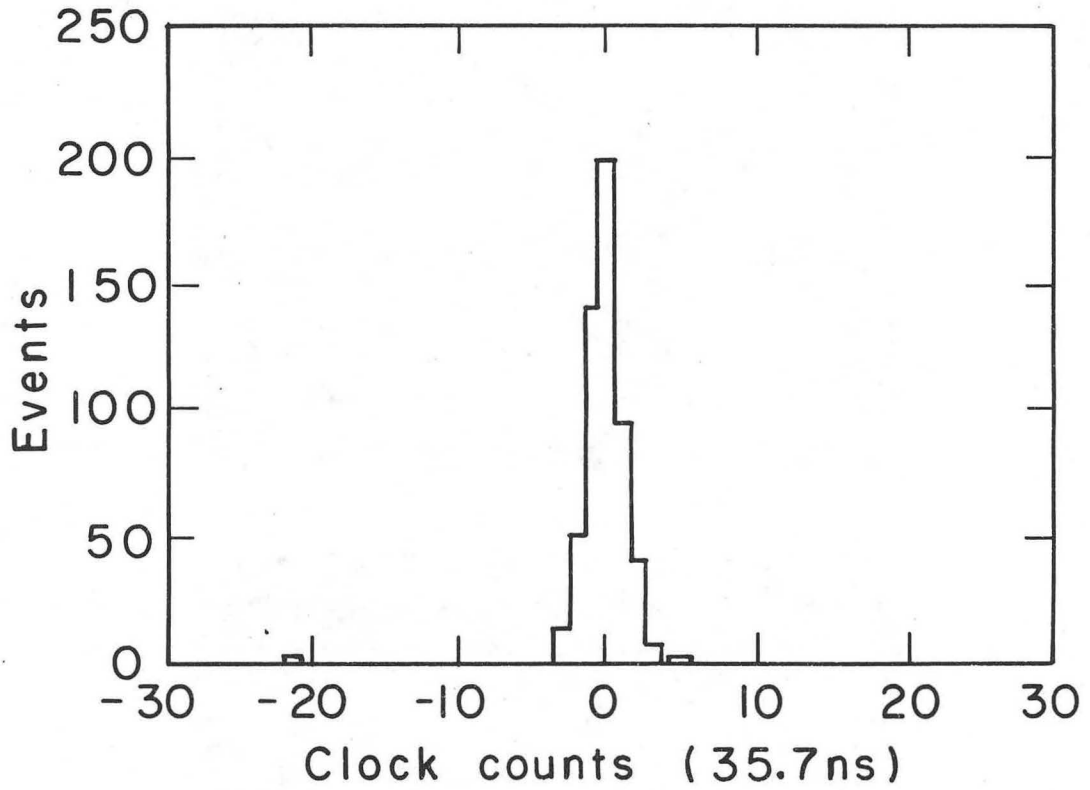


XBL 764-2719

Fig. 11. Difference between predicted and observed times. Divide by $\sqrt{2}$ for single chamber error.

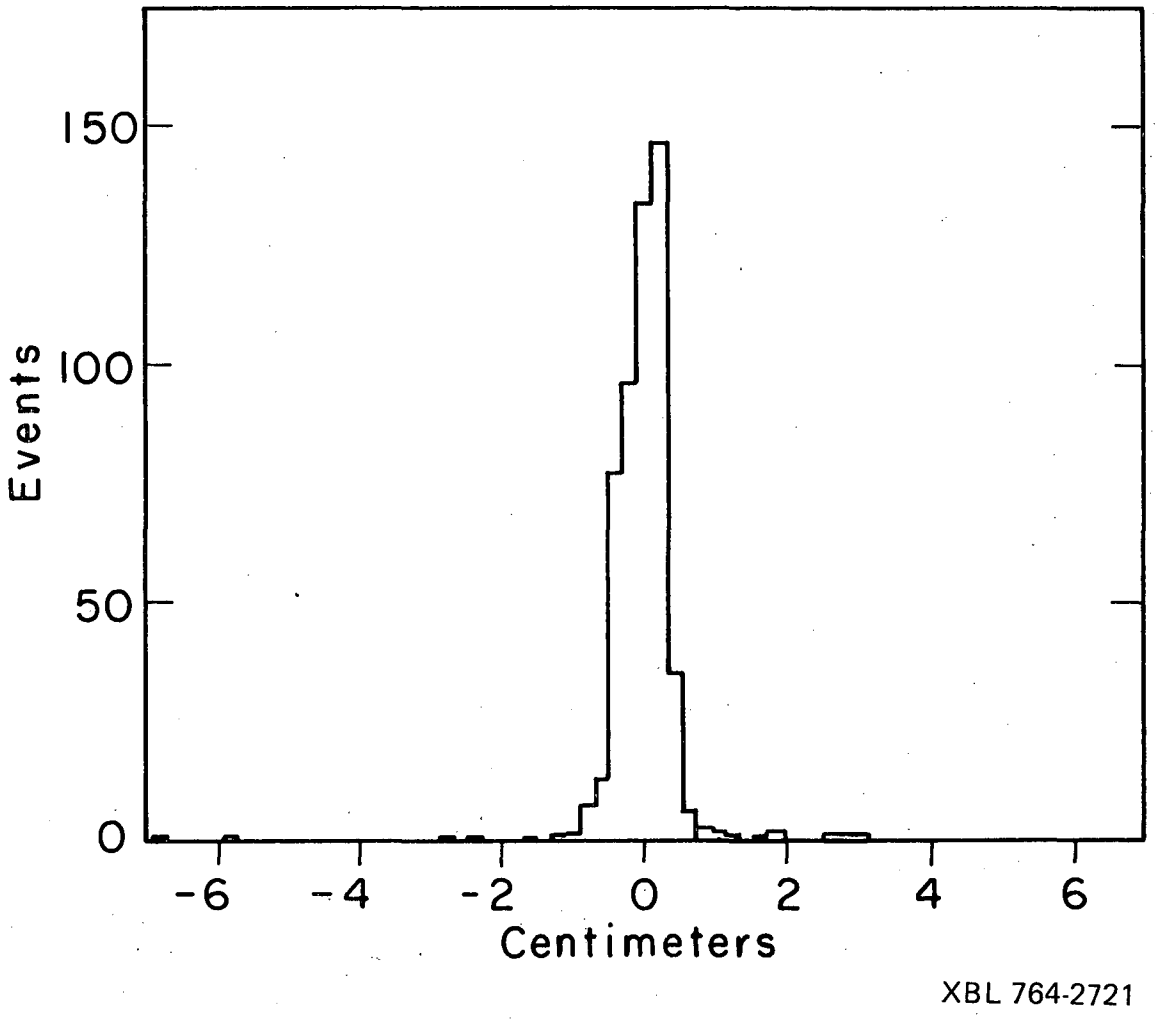


Fig. 12. Difference between predicted and observed values for cathode (X) plane coordinates. Divide by $\sqrt{2}$ for single chamber error.

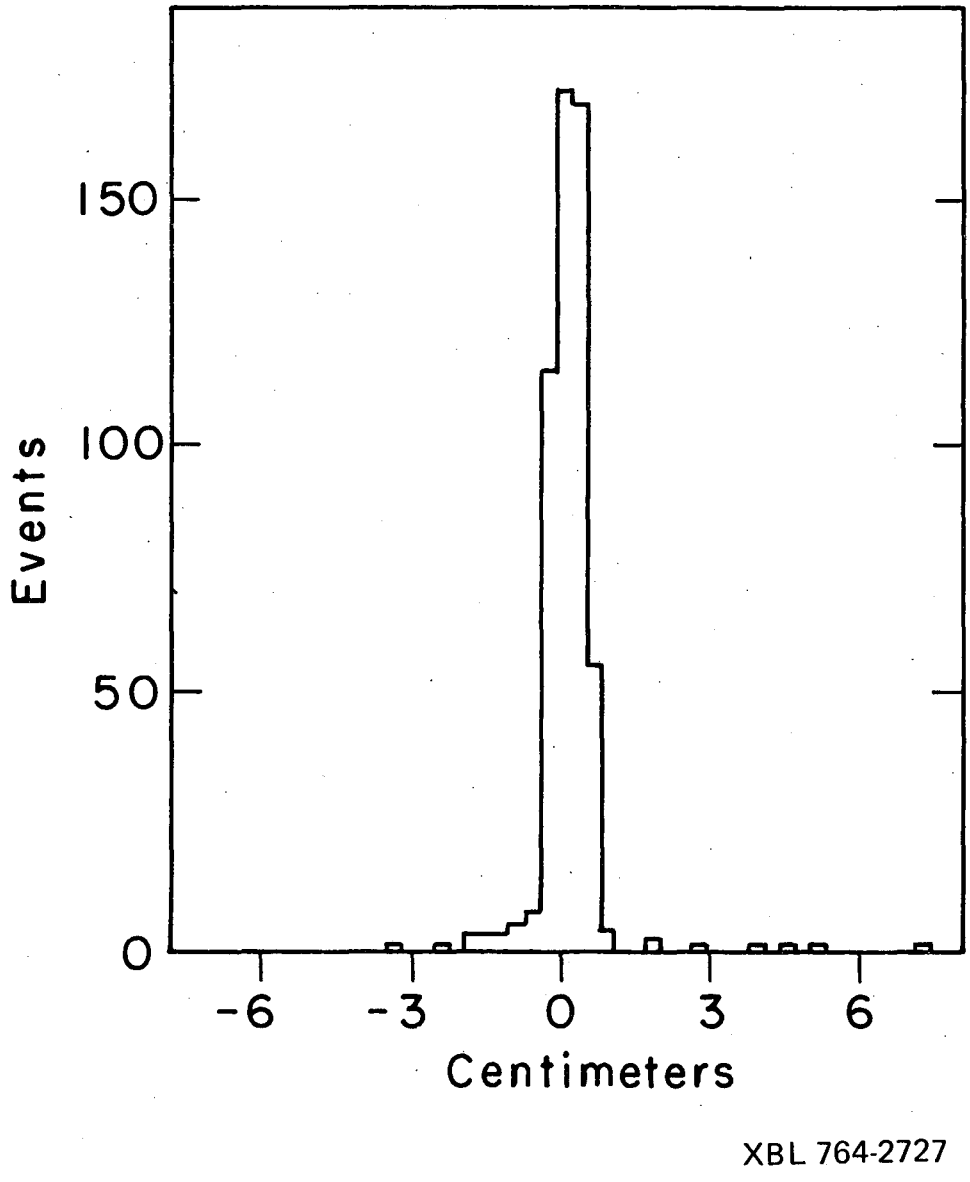


Fig. 13. Difference between predicted and observed values for anode (Y) plane coordinates. Divide by $\sqrt{2}$ for single chamber error.

*TECHNICAL INFORMATION DEPARTMENT*
*LAWRENCE BERKELEY LABORATORY*
*UNIVERSITY OF CALIFORNIA*
*BERKELEY, CALIFORNIA 94720*